

三个单核钌配合物的合成、表征及抗肿瘤活性

张 燕* 杨 艳 温艳珍 贾士芳*
(太原科技大学化学与生物工程学院, 太原 030024)

摘要: 对 3 种单核钌配合物 $[\text{Ru}(\text{bpy})_2(\text{paH})]\text{PF}_6$ (**1**), $[\text{Ru}(\text{dmb})_2(\text{paH})]\text{PF}_6$ (**2**), $[\text{Ru}(\text{phen})_2(\text{paH})]\text{PF}_6$ (**3**) (bpy=2,2'-联吡啶, dmb=4,4'-二甲基-2,2'-联吡啶, phen=菲咯啉, paH=2-吡啶甲酸)进行合成,并通过元素分析、红外、核磁和电喷雾质谱对其进行表征。此外,对配合物进行了光谱学和电化学测试,电化学实验表明 **1~3** 在 0.7~1.0 V 范围内均有 1 个氧化还原峰,说明钌中心发生了氧化还原反应。最后通过 MTT 法(MTT 为 3-(4,5-二甲基噻唑-2)-2,5-二苯基四氮唑溴盐)对配合物进行了体外细胞毒性实验,结果表明:**1~3** 对人乳腺癌细胞、胃癌细胞和肺癌细胞都表现出浓度依赖性,即随着配合物浓度的逐渐增大,细胞的存活率逐渐降低。值得注意的是 **2** 对乳腺癌细胞表现出非常明显的抑制作用($\text{IC}_{50}=2.85 \mu\text{mol}\cdot\text{L}^{-1}$)。

关键词: 单核钌配合物;光谱性质;电化学性质;细胞毒性

中图分类号: O614.82¹

文献标识码: A

文章编号: 1001-4861(2017)06-1035-08

DOI: 10.11862/CJIC.2017.123

Syntheses, Characterization and Antitumor Activity of Three Mononuclear Ruthenium(II) Complexes

ZHANG Yan* YANG Yan WEN Yan-Zhen JIA Shi-Fang*

(School of Chemical and Biological Engineering, Tai Yuan Science and Technology University, Taiyuan 030024, China)

Abstract: Three new mononuclear ruthenium complexes $[\text{Ru}(\text{bpy})_2(\text{paH})]\text{PF}_6$ (**1**), $[\text{Ru}(\text{dmb})_2(\text{paH})]\text{PF}_6$ (**2**) and $[\text{Ru}(\text{phen})_2(\text{paH})]\text{PF}_6$ (**3**) (bpy = 2,2'-bipyridine, dmb = 4,4'-dimethyl-2,2'-bipyridine, phen = phenanthroline, paH = pyridinecarboxylic acid) were synthesized and characterized using elemental analysis, infrared, nuclear magnetic spectroscopy and electrospray ionization mass spectrometry. Their photophysical and electrochemical properties were also studied. The complexes **1~3** undergo metal centered oxidation and the Ru(II)/Ru(III) redox couple peak are in 0.7~1.0 V versus a saturated calomel electrode. The cytotoxicity of these complexes *in vitro* was evaluated using the 3-(4,5-dimethylthiazol-2-yl)-2,5-diphenyltetrazolium bromide(MTT) assay. The results indicated that **1~3** exhibited significant dose-dependent cytotoxicity to human breast cancer (MCF-7), gastric cancer (AGS) and lung cancer (A549) tumour cell lines. It is worth noting that **2** showed excellent antitumor effects in a cellular study (IC_{50} value of $2.85 \mu\text{mol}\cdot\text{L}^{-1}$ for human breast cancer cells *in vitro*).

Keywords: mononuclear ruthenium complexes; spectroscopy property; electrochemistry property; cytotoxicity

0 Introduction

Development of more efficient anticancer drugs with better selectivity but less toxic side effects is

currently an area of intense research in bioinorganic chemistry^[1-2]. Since the discovery of cisplatin by Rosenberg in 1964, more and more attention has been paid to the metal complexes as potential anticancer

收稿日期:2016-12-16。收修改稿日期:2017-04-05。

国家自然科学基金(No.21101121)、湖北省自然科学基金(No.2010CDB01301)和太原科技大学博士启动基金(No.20172005)资助项目。

*通信联系人。E-mail: yanzhang872010@163.com, jiashifang@126.com

drugs^[3-5]. Cisplatin is still used today and is highly effective against testicular and ovarian carcinoma as well as bladder, head and neck tumours^[6]. However, platinum-based anticancer chemotherapy is associated with severe side effects because of poor specificity^[7]. In the case of cisplatin, systemic toxicities like nephrotoxicity, neurotoxicity and ototoxicity inflict serious disorders or injuries on the patients during the treatment, which badly restrict its efficacy^[8]. Many transition metal complexes and small-molecule-based antitumor agents have been developed as new drugs^[9-15]. Among the different metal complexes generating interests, ruthenium complexes have shown great potential and remain the subject of extensive drug discovery efforts, because ruthenium has low energy barrier between its oxidation states and low atomic radius in the transition metal series (0.125 nm) and soluble in water, which are beneficial for its accumulation in cancer tissues^[16]. In the year 1999, NAMI-A (ImH [trans-RuCl₄ (DMSO)(Im)]₂) and in the year 2003, KP1019 (InH [trans-RuCl₄ (In)₂]) was successfully entered into phase I clinical trials for the treatment of metastatic tumors and colon cancers^[17-18]. Now NAMI-A was successfully entered into phase II clinical trials for the treatment of non-small cell lung cancer^[19]. Both of them have their own limitations but in order to promote them as drugs, the way for development of new Ru(II) anticancer complexes is paved. Now the journey of new anticancer drugs starts with ruthenium polypyridyl complexes by overcoming limitations. Recently, some Ru(II) polypyridine complexes as antitumor agents were reported by our group^[20-21]. A large number of ruthenium(II) complexes containing a {Ru(bpy)₂} (bpy=2,2'-bipyridine) moiety with a variety of ancillary bidentate ligands have been reported^[22-27]. Among these ligands a class belongs to the carboxylic acid ligands. Such ligands are of particular interest as they can play important roles in deciding the physical properties and chemical properties of the complex due to the possibility of redox electron delocalization between the metal ion and the ligand.

In this study, three new ruthenium(II) complexes

containing the ancillary ligand pyridinecarboxylic acid were synthesized and characterized using elemental analysis, IR, ¹H NMR spectroscopy and electrospray ionization mass spectrometry (ESI-MS). The UV-Vis absorption spectroscopy, fluorescence spectroscopy and electrochemical behavior of them were also studied. Moreover, these antitumor effects were investigated in vitro, and **2** exhibited the best inhibitory effect among three complexes.

1 Experimental

1.1 Materials and instrument

All reagents and solvents were of commercial origin and were used without further purification unless otherwise noted. Ultrapure Milli-Q water was used in all experiments. Dimethyl sulfoxide (DMSO) and RPMI 1640 were purchased from Sigma. MCF-7 (human breast cancer), AGS (human gastric carcinoma) and A549 (human lung cancer) cell lines were purchased from the American Type Culture Collection. RuCl₃·3H₂O, 2,2'-bipyridyl (bpy), 4,4'-dimethyl-2,2'-bipyridine (dmb), phenanthroline(phen) and 2-pyridinecarboxylic acid (pH) were purchased from the Wuhan Shenshi Huagong, [Ru(L)₂Cl₂]·2H₂O (L=bpy, dmb and phen) were synthesized and purified according to literature methods^[28].

Microanalysis (C, H, and N) was conducted with a PerkinElmer 240Q elemental analyzer. Electrospray ionization mass spectra were recorded with an LCQ system (Finnigan MAT, USA) using CH₃OH as the mobile phase. 300 MHz ¹H NMR spectroscopic measurements were performed on a Bruker AM-300 NMR spectrometer, using DMSO-d₆ as solvent and TMS (SiMe₄) as an internal reference at 25 °C. Infrared spectra were recorded on a Perkin-Elmer Spectrum FTIR spectrometer using KBr pellets. Solution electronic absorption and emission spectra were recorded on Shimadzu 3100 spectrophotometer in acetonitrile and Shimadzu RF-5301 PC spectrofluorometer, respectively. Differential pulse voltammetry (DPV) was done with a CHI 630E instrument in a three-electrode cell with a pure Ar gas inlet and outlet. The working electrode and counter

electrode were Pt electrode, and the reference electrode was a saturated calomel electrode (SCE). The experiments were carried out in the presence of CH₃CN. DPV experiments were performed with a scan rate of 20 mV·s⁻¹.

1.2 Synthesis of Ru complexes

[Ru(bpy)₂(paH)]PF₆(**1**): AgNO₃ (0.17 g, 1.0 mmol) was added to an ethanol solution of [Ru(bpy)₂Cl₂]·2H₂O (0.26 g, 0.5 mmol). After refluxing for 30 min and filtering to remove the deposited AgCl, the filtrate was added to an ethanol solution (30 mL) of 2-pyridinecarboxylic acid (0.06 g, 0.5 mmol) and NaOH (0.02 g, 0.5 mmol). The mixture was refluxed for 12 h under N₂, and the resulting brown red solution was evaporated to 5 mL. To this solution, excess KPF₆ was added and a brown red solid precipitated. This solid was collected by filtration, washed thoroughly with water and dried in vacuum over P₂O₅. The purification of the complex was performed on a neutral aluminium oxide column. The first moving brown red band was eluted with dichloromethane containing 5% (V/V) acetone. This was collected and evaporated. The solid thus obtained was recrystallized from acetone-diethylether (2:1). Yield: 62%. Anal. Calcd. for C₂₆H₂₀N₅O₂PF₆Ru (%): C, 45.88; H, 2.94; N, 10.29. Found(%): C, 45.83; H, 2.97; N, 10.27. ¹H NMR (300 MHz, DMSO-d₆): δ 7.36 (2H, d, *J*=9.0 Hz), 7.50(2H, m), 7.60(2H, d, *J*=6.0 Hz), 7.78(1H, m), 7.90(1H, d, *J*=3.0 Hz), 7.95~7.99(4H, m), 8.17(2H, m), 8.70~8.78 (4H, m), 8.81(2H, d, *J*=9.0 Hz). IR (KBr, cm⁻¹): 1 605, 1 580, 1 508, 1 441, 1 341, 1 263, 1 240, 1 182, 1 148, 1 130, 1 020, 901, 839, 760, 727, 658, 556. ESI-MS: *m/z* 443.6 ([Ru(bpy)₂·CH₃O]⁺), 536.0 ([M-PF₆]⁺).

[Ru(dmb)₂(paH)]PF₆(**2**): The method used to synthesize **2** was exactly similar to the **1**, except that [Ru(dmb)₂Cl₂]·2H₂O was used. Yield: 78%. Anal. Calcd. for C₃₀H₂₈N₅O₂PF₆Ru (%): C, 48.91; H, 3.80; N, 9.51. Found (%): C, 48.93; H, 3.77; N, 9.52. ¹H NMR (300 MHz, DMSO-d₆): δ 2.45(6H, s), 2.56(6H, s), 7.19 (2H, m), 7.40~7.49 (3H, m), 7.61 (2H, d, *J*=6.0 Hz), 7.69(1H, d, *J*=6.0 Hz), 7.96~8.01(3H, m), 8.49(1H, d, *J*=6.0 Hz), 8.58 (2H, m), 8.64 (2H, d, *J*=6.0 Hz). IR

(KBr, cm⁻¹): 1 708, 1 621, 1 486, 1 371, 1 228, 1 122, 1 016, 843, 766, 690, 555. ESI-MS: *m/z* 592.1 ([M-PF₆]⁺).

[Ru(phen)₂(paH)]PF₆(**3**): The method used to synthesize **3** was similar to the **1**, except that [Ru(phen)₂Cl₂]·2H₂O was used. Yield: 67%. Anal. Calcd. for C₃₀H₂₀N₅O₂PF₆Ru (%): C, 49.45; H, 2.75; N, 9.62. Found (%): C, 49.48; H, 2.69; N, 9.65. ¹H NMR (300 MHz, DMSO-d₆): δ 7.37 (1H, m), 7.47 (1H, d, *J*=3.0 Hz), 7.59(2H, m), 7.86(1H, d, *J*=6.0 Hz), 7.94(2H, m), 8.01~8.06 (3H, m), 8.12 (2H, m), 8.33~8.38 (4H, m), 8.57 (2H, m), 8.81 (2H, d, *J*=9.0 Hz). IR (KBr, cm⁻¹): 1 620, 1 420, 1 324, 1 141, 834, 719, 555. ESI-MS: *m/z* 584.1 ([M-PF₆]⁺).

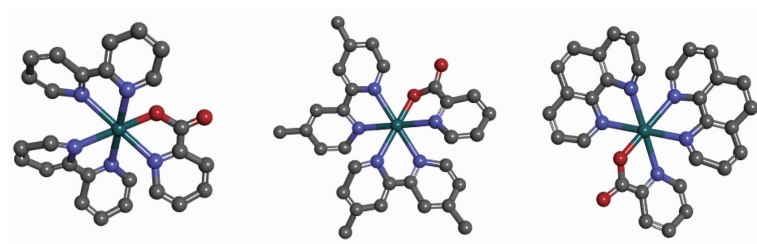
1.3 Methods

Standard MTT assay procedures were used [29]. Cells were placed in 96-well microassay culture plates (8×10³ cells per well) and grown overnight at 37 °C in a 5%(V/V) CO₂ incubator. The complexes tested were then added to the wells to achieve final concentrations ranging from 0.39 to 100 μmol·L⁻¹. Control wells were prepared by addition of culture medium (200 μL). The plates were incubated at 37 °C in a 5%(V/V) CO₂ incubator for 48 h. On completion of the incubation, stock MTT dye solution (20 μL, 5 mg·mL⁻¹) was added to each well. After 4 h, 150 μL dimethylsulfoxide (DMSO) was added to solubilize the MTT formazan. The optical density of each well was then measured with a microplate spectrophotometer at a wavelength of 490 nm. The IC₅₀ values were determined by plotting the percentage viability versus the concentration and reading off the concentration at which 50% of the cells remained viable relative to the control. Each experiment was repeated at least three times to obtain the mean values. Three different tumor cell lines were the subjects of this study: MCF-7 (human breast carcinoma), AGS (human gastric carcinoma), and A549(human lung carcinoma).

2 Results and discussion

2.1 Design and synthesis

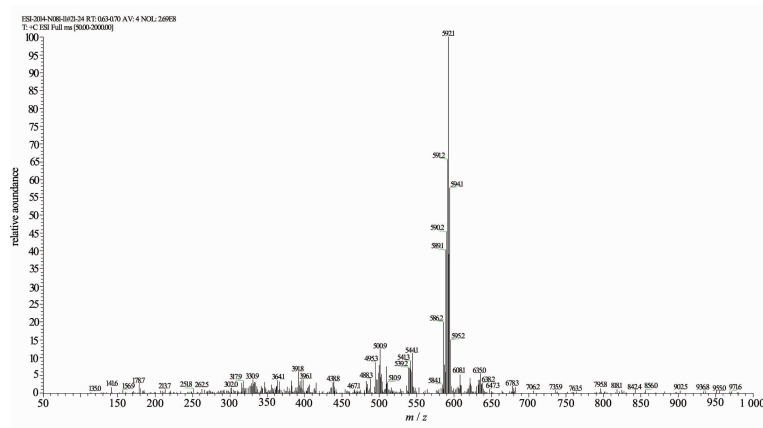
All three complexes (Scheme 1) were synthesized using the general, previously reported method. In

Scheme 1 Structures of the complexes **1**, **2** and **3** omitting the anion PF_6^-

order to obtain the pure products, chromatographic purification was necessary on a neutral aluminum oxide column, and the complexes were afforded in good yields. The crystals of the complexes were not obtained, however, ESI-MS and ^1H NMR helped us to determine their structure in solution.

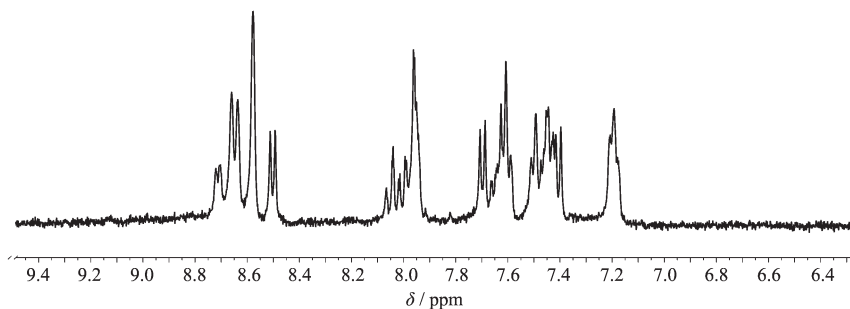
In the ESI-MS of the complexes **1**, **2** and **3**, the peaks at m/z 536.0, 592.1 and 584.1 were designated

to the species $[\text{Ru}(\text{bpy})_2(\text{paH})]^+$, $[\text{Ru}(\text{dmb})_2(\text{paH})]^+$ and $[\text{Ru}(\text{phen})_2(\text{paH})]^+$, respectively. A representative spectrum for **2** was shown in Fig.1 (ESI-MS spectra of **1** and **3** are in supporting information). The observed peaks revealed that coordination cations of the three complexes were formed by one Ru(II) center, one paH, and two bpy (or dmb, or phen), and the coordination cations were stable in the solution.

Fig.1 Electrospray mass spectrum of complex **2** in CH_3OH

The ^1H NMR spectra of the three complexes were recorded in $\text{DMSO}-d_6$. The absence of free carboxyl proton ($\delta > 10$) in all spectra confirm the complexation through the CO-O. The aromatic region of each spectrum was very complicated due to their similar

electronic environments of many aromatic hydrogen atoms, and their signals were in a narrow regions shift range ($\delta = 7.3 \sim 8.9$). The number of aromatic proton signals was consistent with the number of protons of the molecular formula. However, it is difficult to

Fig.2 ^1H NMR spectrum in $\text{DMSO}-d_6$ of complex **2**

assign all the individual signals, respectively. A representative ^1H NMR spectrum of **2** was shown in Fig.2 (^1H NMR spectra of **1** and **3** are in supporting information). In their solid state, elemental analysis data were satisfactory with the general formula including the PF_6^- anion.

2.2 Infrared spectroscopy

Infrared spectra of the complexes do not display any band near $3\,300\text{ cm}^{-1}$, which suggested that the $-\text{COOH}$ of paH was deprotonated in the complexes. The free carboxylic acid displayed a peak near $1\,650\text{ cm}^{-1}$ that was assigned to the $\text{C}=\text{O}$ group. A medium to strong peak was observed in the range of $1\,590\sim 1\,640\text{ cm}^{-1}$ for all the three complexes. This peak might originated from the metal-coordinated $\text{C}=\text{O}$ group of paH. The strong and sharp peak displayed by the complexes in the range of $1\,420\sim 1\,440\text{ cm}^{-1}$ is likely to be associated with the $\text{C}=\text{N}$ fragments of the ancillary ligands. The presence of PF_6^- in each complex is indicated by a strong peak at 840 cm^{-1} ^[30] (IR spectra of **1** and **3** are in supporting information).

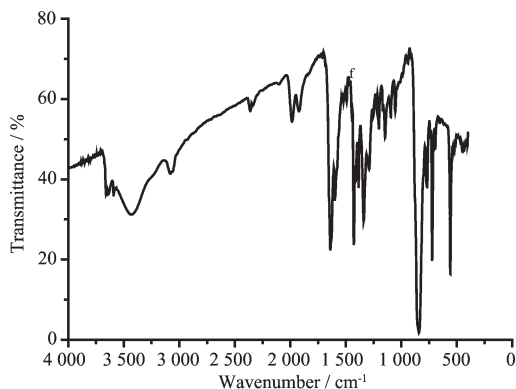


Fig.3 Infrared spectrum (KBr pellet) of complex **2**

2.3 Electronic absorption spectra

The absorption spectra of the three complexes were recorded in acetonitrile (Fig.4). With the exception of **3**, the spectral profiles of the other

complexes were very similar. Complexes **1** and **2** displayed three absorptions peaks at $490\sim 495\text{ nm}$, $360\sim 365\text{ nm}$ and $285\sim 295\text{ nm}$, while **3** displayed two absorptions peaks at $435\sim 445\text{ nm}$ and $260\sim 265\text{ nm}$. These absorption peaks for **3** were significantly blue shifted compared with the other complexes. The bands at 260, 290 and 360 nm are attributed to intraligand $\pi \rightarrow \pi^*$ transitions. The lowest energy bands, approximately 440 and 490 nm, are assigned to metal-ligand charge transfer (MLCT) ($d_{\text{Ru}} \rightarrow \pi^*$)^[31].

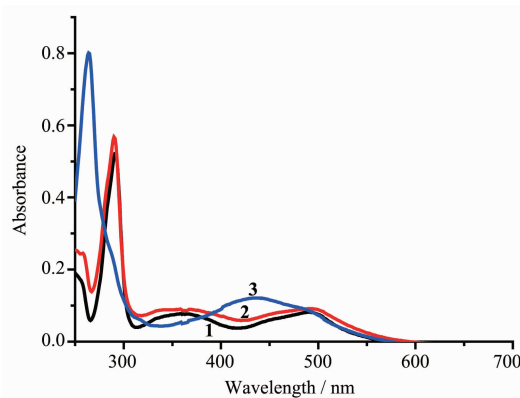


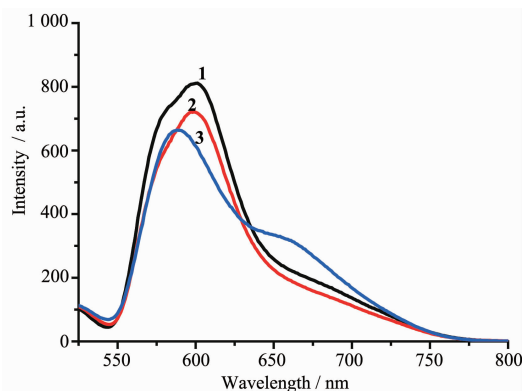
Fig.4 Absorption spectra of **1~3** in acetonitrile ($10\text{ }\mu\text{mol}\cdot\text{L}^{-1}$)

2.4 Luminescence spectra studies

The emission spectral data (wavelength of excitation and emission) are presented in Table 1. All the measurements were made with solutions deoxygenated by purging Ar. The excitation spectra of **1~3** were monitored at the emission maxima of each complex at room temperature. Complexes **1~3** upon excitation onto their excitation maxima exhibited an emission band at 602, 599 and 587 nm, respectively. The emission profile and emission maxima were similar and independent of the excitation wavelength. What is noteworthy is that **3** has a shoulder peak at 661nm. The electronic emission spectra of the **1~3** are presented in Fig.5.

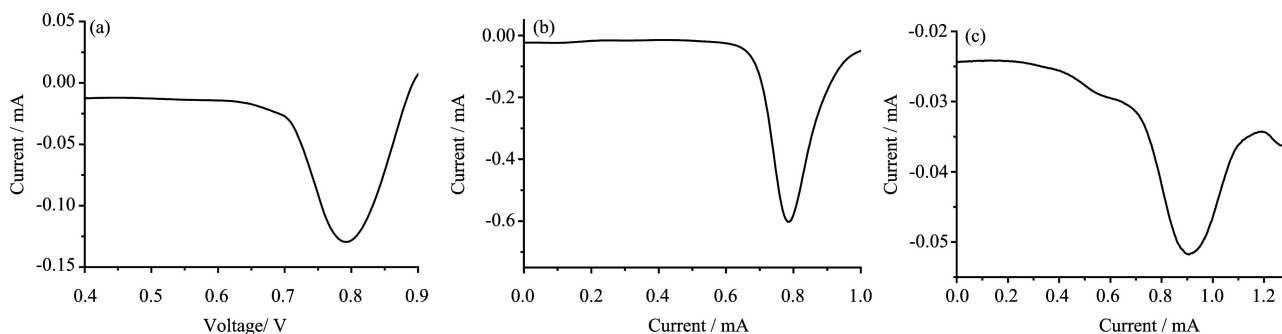
Table 1 Electronic spectroscopic data of complexes **1~3** in CH_3CN

Complex	Absorption	Emission	
	$\lambda_{\text{max}} / \text{nm}$ ($\epsilon / (\text{dm}^3 \cdot \text{mol}^{-1} \cdot \text{cm}^{-1})$)	$\lambda_{\text{ex}} / \text{nm}$	$\lambda_{\text{em}} / \text{nm}$
1	291(5.17×10^4), 364(7.5×10^3), 492(7.8×10^3)	450	602
2	289(5.63×10^4), 362(8.7×10^3), 492(9.0×10^3)	452	599
3	263(7.97×10^4), 440(1.19×10^5)	452	587, 661



$c=10 \mu\text{mol}\cdot\text{L}^{-1}$, $\lambda_{\text{ex}}=450 \text{ nm}$

Fig.5 Emission spectra of **1**~**3** in acetonitrile



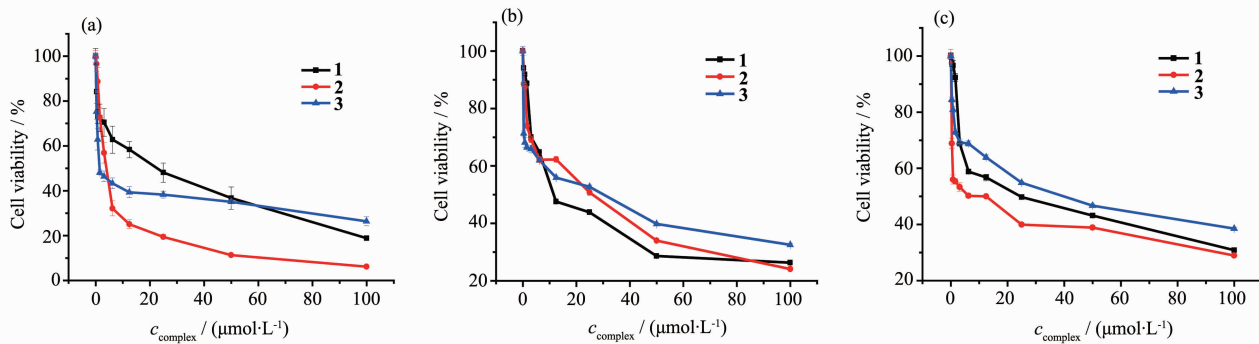
$0.1 \text{ mol}\cdot\text{L}^{-1} \text{ NBu}_4\text{ClO}_4$; Scan rate= $20 \text{ mV}\cdot\text{s}^{-1}$

Fig.6 DPV of **1**(a), **2**(b) and **3**(c) in CH_3CN solution

2.6 In vitro cytotoxicity

The MCF-7 (human breast cancer cell line), AGS (human gastric cancer cell line) and A549 (human gastric cancer cell line) cells were treated with different concentrations of paH, $[\text{Ru}(\text{bpy})_2\text{Cl}_2]\cdot 2\text{H}_2\text{O}$, $[\text{Ru}(\text{dmb})_2\text{Cl}_2]\cdot 2\text{H}_2\text{O}$, $[\text{Ru}(\text{phen})_2\text{Cl}_2]\cdot 2\text{H}_2\text{O}$, cisplatin, **1**, **2** and **3** for 48 h. The cytotoxicity of these compounds towards the aforementioned cell lines was evaluated using the MTT

method. Culture medium containing 0.05% DMSO was used as the negative control. After treatment of three cell lines for 48 h with these compounds in a range of concentrations ($0.39\sim 100 \mu\text{mol}\cdot\text{L}^{-1}$), the percentage inhibition of growth of the cancer cells was determined. The cell viabilities (%) vs concentrations obtained with continuous exposure for 48 h are depicted in Fig.7, and the IC_{50} values are listed in Table 2. It was found that



Each point is mean \pm standard error obtained from three independent experiments

Fig.7 Cell viability of **1**~**3** toward proliferation of MCF-7 (a), AGS (b) and A549 (c) cells *in vitro*

2.5 Electrochemistry analysis

The differential pulse voltammetry (DPV) technique is employed to obtain well-resolved potential information, while the individual redox processes for the multinuclear complexes are poorly resolved in the cyclic voltammetry experiment, in which individual $E_{1/2}$ potentials cannot be easily or accurately extracted from the data. Differential pulse voltammetry (DPV) of the **1**~**3** were recorded in acetonitrile, the voltammograms were shown in Fig.6. All the three complexes exhibit one oxidation in the range of 0.7~1.0 V, which assigned to Ru(II)/Ru(III) couple^[32-33].

Table 2 IC_{50} value of Ru-complexes, paH and cisplatin against selected cell lines

Compound	$IC_{50} / (\mu\text{mol} \cdot \text{L}^{-1})$		
	MCF-7	AGS	A549
paH	>100	>100	>100
$[\text{Ru}(\text{bpy})_2\text{Cl}_2] \cdot 2\text{H}_2\text{O}$	88.23 ± 1.6	92.53 ± 1.3	90.59 ± 1.05
$[\text{Ru}(\text{dmb})_2\text{Cl}_2] \cdot 2\text{H}_2\text{O}$	75.12 ± 0.95	88.07 ± 0.65	85.37 ± 1.55
$[\text{Ru}(\text{phen})_2\text{Cl}_2] \cdot 2\text{H}_2\text{O}$	93.87 ± 2.06	95.46 ± 0.88	>100
1	25.82 ± 3.6	24.12 ± 1.02	22.94 ± 0.98
2	2.85 ± 4.5	15.08 ± 0.24	11.98 ± 0.82
3	4.29 ± 2.9	28.98 ± 0.55	38.52 ± 0.53
cisplatin	28.69 ± 0.93	25.32 ± 1.12	23.93 ± 0.99

the IC_{50} value of paH was more than $100 \mu\text{mol} \cdot \text{L}^{-1}$, the IC_{50} values of $[\text{Ru}(\text{bpy})_2\text{Cl}_2] \cdot 2\text{H}_2\text{O}$, $[\text{Ru}(\text{dmb})_2\text{Cl}_2] \cdot 2\text{H}_2\text{O}$, $[\text{Ru}(\text{phen})_2\text{Cl}_2] \cdot 2\text{H}_2\text{O}$ were greater than **1~3**, respectively. The cytotoxicity of the complexes was found to be concentration dependent. The cell viability decreased with increasing concentrations of the complexes. As shown in Table 2, it was clear that **2** was generally the most active complex and exhibited low IC_{50} values, particularly at the concentration of $2.85 \mu\text{mol} \cdot \text{L}^{-1}$ for the MCF-7 cells at 48 h, compared with that of cisplatin, $28.69 \mu\text{mol} \cdot \text{L}^{-1}$. The cytotoxicity of **1** was higher than that of **3** towards AGS and A549 cells, and there was an opposite phenomenon in the MCF-7 cells, but these IC_{50} values were obviously higher than those of **2** in all three cell lines. Overall, among these complexes, **2** exhibited the highest cytotoxicity in MCF-7, AGS and A549 cells. A series of mononuclear ruthenium complexes $[\text{Ru}(\text{bpy})_2(\text{salH})]\text{PF}_6$ (Ru1), $[\text{Ru}(\text{dmb})_2(\text{salH})]\text{PF}_6$ (Ru2) and $[\text{Ru}(\text{phen})_2(\text{salH})]\text{PF}_6$ (Ru3), where salH = salicylaldehyde, were reported by our group^[34]. The A549, BGC823 and MDA-MB-231 cells were treated with different concentrations of Ru1, Ru2 and Ru3. It was found that Ru2 was generally the most active complex and exhibited low IC_{50} values, particularly at the concentrations of 7.97 and $3.60 \mu\text{mol} \cdot \text{L}^{-1}$ for the A549 and BGC823 cells respectively for 48 h. The activity of these two series of complexes as anti-cancer drugs is consistent. When the ancillary ligand is dmb (dmb = 4,4'-dimethyl-2,2'-bipyridine), the cytotoxicity of complex is the largest.

2.7 Octanol-water partition coefficients

The activity of anticancer drugs is often related to their lipophilic character, and the resulting hydrophobicity may contribute to an increased uptake of the complex by the cells, thereby enhancing the antiproliferative activity^[35-39]. The standard octanol-water partition coefficient ($\lg P$) was determined for **1~3**: -1.5 for **1**; -1.2 for **2**; -1.9 for **3**. From the results, complex **2** is more lipophilic than **1** and **3**. For the ruthenium complexes, the anticancer activity directly related to the $\lg P$, because of activity increasing with the increase in lipophilicity. This suggests that lipophilicity is an important determinant of activity, but only to the level that allows the ruthenium complex to easily diffuse across the cellular membrane^[40].

3 Conclusions

A series of new mononuclear Ru(II) complexes were synthesized and characterized using elemental analysis, IR, ESI-MS and ^1H NMR techniques. Absorption spectra, luminescent properties and electrochemical behavior of the complexes were also studied. Complexes **1~3** exhibit the spin-allowed singlet metal-to-ligand charge transfer transition at approximate 490 and 440 nm and Ru(II) metal centered emission at around 600 nm in solution at room temperature. Moreover, **1~3** undergo metal centered oxidation and the Ru(II)/Ru(III) redox couple are 0.7~1.0 V (vs SCE). In vitro cytotoxic assays of the complexes were studied, and the results indicate that Ru(II) complexes

show significant dose-dependent cytotoxicity to breast cancer (MCF-7), gastric cancer (AGS) and lung cancer (A549) tumour cell lines, and **2** shows excellent anti-tumor effects in a cellular study (IC_{50} value of $2.85 \mu\text{mol} \cdot \text{L}^{-1}$ for MCF-7 *in vitro*). This result reveals that **2** might be a potential anticancer agent that could improve on the efficacy of common anticancer therapies, such as platinum-based drugs.

Supporting information is available at <http://www.wjhxxb.cn>

References:

- [1] Makhubela B C E, Meyer M, Smith G S. *J. Organomet. Chem.*, **2014**, **772**:229-241
- [2] Alagesan M, Sathyadevi P, Krishnamoorthy P, et al. *Dalton Trans.*, **2014**, **43**:15829-15840
- [3] Nguyen T D, Duong T T, Le T P Q, et al. *Med. Chem. Res.*, **2011**, **20**:790-793
- [4] Li G Y, Du K J, Wang J Q, et al. *J. Inorg. Biochem.*, **2013**, **119**:43-53
- [5] Pinato O, Musetti C, Farrell N P, et al. *J. Inorg. Biochem.*, **2013**, **122**:27-37
- [6] Reedijk J. *Chem. Commun.*, **1996**, 801-806
- [7] McWhinney S R, Goldberg R M, McLeod H L. *Mol. Cancer Ther.*, **2009**, **8**:10-16
- [8] Liu Y J, Zeng C H, Liang Z H, et al. *Eur. J. Med. Chem.*, **2010**, **45**:3087-3095
- [9] Morais T S, Santos F, C  rte-Real L, et al. *J. Inorg. Biochem.*, **2013**, **122**:8-17
- [10] Liu Y J, Liang Z H, Li Z Z, et al. *J. Organomet. Chem.*, **2011**, **696**:2728-2735
- [11] Jaividhya P, Dhivya R, Akbarsha M A, et al. *J. Inorg. Biochem.*, **2012**, **114**:94-105
- [12] Abdi K, Hadadzadeh H, Weil M, et al. *Polyhedron*, **2012**, **31**:638-648
- [13] Li M J, Lan T Y, Cao X H, et al. *Dalton Trans.*, **2014**, **43**: 2789-2798
- [14] Govender P, Edafe F, Makhubela B C E, et al. *Inorg. Chim. Acta*, **2014**, **409**:112-120
- [15] Kalidasan M, Forbes S, Mozharivskyj Y, et al. *Inorg. Chim. Acta*, **2014**, **421**:349-358
- [16] Rademaker-Lakhai J M, Bongard D, Pluim D. *Clin. Cancer Res.*, **2004**, **10**:3717-3727
- [17] Hartinger C G, Jakupcica M A, Zorbas-Seifrieda S, et al. *Chem. Biodivers.*, **2008**, **5**:2140-2155
- [18] Lentz F, Drescher A, Lindauer A, et al. *Anti-Cancer Drugs.*, **2009**, **20**:97-103
- [19] Leijen S, Burgers S A, Baas P, et al. *Invest. New Drugs.*, **2015**, **33**:201-214
- [20] Zhang Y, Lai L, Cai P, et al. *New J. Chem.*, **2015**, **39**:5805-5812
- [21] Zhang Y, Hu P C, Cai P, et al. *RSC Adv.*, **2015**, **5**:11591-11598
- [22] Roy S, Maheswari P U, Golobic A, et al. *Inorg. Chim. Acta*, **2012**, **393**:239-245
- [23] Karki S S, Thota S, Darj S Y, et al. *Bioorg. Med. Chem.*, **2007**, **15**:6632-6641
- [24] Srishailam A, Kumar Y P, Reddy P V, et al. *J. Photochem. Photobiol. B*, **2014**, **132**:111-123
- [25] Stringer T, Therrien B, Hendricks D T, et al. *Inorg. Chem. Commun.*, **2011**, **14**:956-960
- [26] Garza-Ortiz A, Maheswari P U, Siegler M, et al. *New J. Chem.*, **2013**, **37**:3450-3460
- [27] Lin G J, Jiang B, Xie Y Y, et al. *J. Biol. Inorg. Chem.*, **2013**, **18**:873-882
- [28] Sullivan B P, Salmon D J, Meyer T J. *Inorg. Chem.*, **1978**, **17**:3334-3341
- [29] Mosmann T. *J. Immunol. Methods*, **1983**, **65**:55-63
- [30] Pal S. Z. *Anorg. Allg. Chem.*, **2002**, **628**:2091-2098
- [31] Constable E C, Housecro C E, Kopecky P, et al. *Polyhedron*, **2013**, **64**:38-44
- [32] Pal S, Pal S. *Inorg. Chem.*, **2001**, **40**:4807-4810
- [33] ZHANG Yan(张燕), XIONG Bi(熊碧), CAI Ping(蔡苹), et al. *Chinese J. Inorg. Chem.*(无机化学学报), **2012**, **28**(11): 2437-2443
- [34] Hu P C, Wang Y, Zhang Y, et al. *RSC Adv.*, **2016**, **6**: 29963-29976
- [35] Mendoza-Ferri M G, Hartinger C G, Mendoza M A, et al. *J. Med. Chem.*, **2009**, **52**:916-925
- [36] Giannini F, Paul L E H, Furrer J, et al. *New J. Chem.*, **2013**, **37**:3503-3511
- [37] Mulyana Y, Weber D K, Buck D P, et al. *Dalton Trans.*, **2011**, **40**:1510-1523
- [38] Gorle A K, Ammit A J, Wallace L, et al. *New J. Chem.*, **2014**, **38**:4049-4059
- [39] DeBerardinis R J, Lum J J, Hatzivassiliou G, et al. *Cell Metab.*, **2008**, **7**:11-20
- [40] Gorle A K, Feterl M, Warner J M, et al. *Dalton Trans.*, **2014**, **43**:16713-16725